SUBSTRATE HEATER DESIGN INVESTIGATION FOR UNIFORM TEMPERATURE IN A COLD-WALL LOW PRESSURE REACTOR

Susan P. Krumdieck
Department of Mechanical Engineering
Private Bag 4800
University of Canterbury
Christchurch 8004
NEW ZEALAND

(Tel) +64 3 364 2987 x7249
(Fax) +64 3 364 2078
Susan.Krumdieck@canterbury.ac.nz

Hyung-Chul Jung
Department of Mechanical Engineering
Private Bag 4800
University of Canterbury
Christchurch 8004
NEW ZEALAND

Keywords:

Heater Design
Heat Transfer
Numerical Analysis
Temperature Uniformity
Optimization

SUBSTRATE HEATER DESIGN INVESTIGATION FOR UNIFORM TEMPERATURE IN A COLD-WALL LOW PRESSURE REACTOR

Susan P. Krumdieck and Hyung-Chul Jung

Department of Mechanical Engineering, University of Canterbury
Christchurch, NEW ZEALAND

Abstract

The critical function of a CVD heating system is to produce a uniform temperature distribution across the surface of the substrate wafer or object. The most challenging system for low-cost heater design is the cold-wall reactor. Secondary considerations include the temperature of other exterior surfaces, materials, commercial heater availability, scalability, and cost. A low cost design was investigated for a wafer heater in research-scale reactors. Numerical modelling and optimization results are confirmed with thermography experiments and demonstrate the relationship between temperature uniformity and design parameters. Heaters with incorporated refractory materials and radiation shielding have the best susceptor temperature uniformity.

INTRODUCTION

The local thin film thickness, composition and microstructure of a thin film are strongly influenced by a complex interaction of transport phenomena, chemical reaction thermodynamics and kinetics, and surface diffusion and crystal growth. All of these processes depend on the temperature distribution throughout the reactor, in the deposition zone, and across the substrate surface (1). At higher pressures and high substrate temperatures in cold-wall reactors, the three dimensional velocity and temperature distributions throughout the reactor pose serious process control problems (2,3). Hot wall reactors have better thermal profile control, but parasitic deposition on hot walls and surfaces reduces precursor conversion efficiency (4).

Design of CVD heaters is not a routine activity among researchers. A survey of CVD handbooks provides little assistance for in-house construction of a research-scale system (5). Lugscheider discusses the impact of possible heating modes on microstructure (6). Campion gives a description of the widely used projector bulb concept (7). Inameti describes a conductive heater design which provides 750^{o}C at 200W by employing radiative shielding (8). A major thrust of our research is the design for manufacturing of PP-MOCVD, thus we have undertaken a study of heater design for single substrates.

Commercial heater assemblies are available, mainly from PVD and PLD equipment suppliers. The general design is a meander or spiral shaped resistance heating element made from pyrolytic graphite or tungsten, in a shielded metal case or potted ceramic plate, inside a housing made of high temperature metals such as molybdenum or tantalum, often with water cooling jackets. Sono-Tek, Inc. (www.sono-tek.com) builds

PP-MOCVD R&D systems for two-inch wafers (9). Pyrolytic boron-nitride heaters have been specially made for this system by Advanced Ceramics (now GE) at significant cost. Our research efforts include determining scaling relations for design of industrial scale PP-MOCVD. In constructing larger scale equipment, our dilemma is to design and build our own CVD equipment from available components and materials at very low cost. This paper presents modelling and analysis of stainless steel heaters we developed to study the heater design for surface temperature uniformity. The heater was modelled and optimized using ANSYS numerical heat transfer package, and the optimal design was verified through experiments on a prototype, using a LAND infrared camera. The final design wafer heater has a thick stainless steel body, and relatively thick shields, with surface temperature uniformity of $\Delta T = 4^{o}C$ and $371^{o}C$ surface temperature at 100W power at 10^{-3} Torr reactor pressure.

HEAT TRANSFER MODEL

The steady state heat diffusion equation was solved for the temperature distribution in the heater body, $T_{(x,y,z)}$, subject to the conditions of our low-pressure cold-wall reactor, as shown in Figure 1. Heat transfer from the outside of the heater body in a vacuum is dominated by radiation exchange between reactor surfaces and transmission through glass to the surroundings. The control volume form of the energy equation for each isotropic solid area in the heater has the general form:

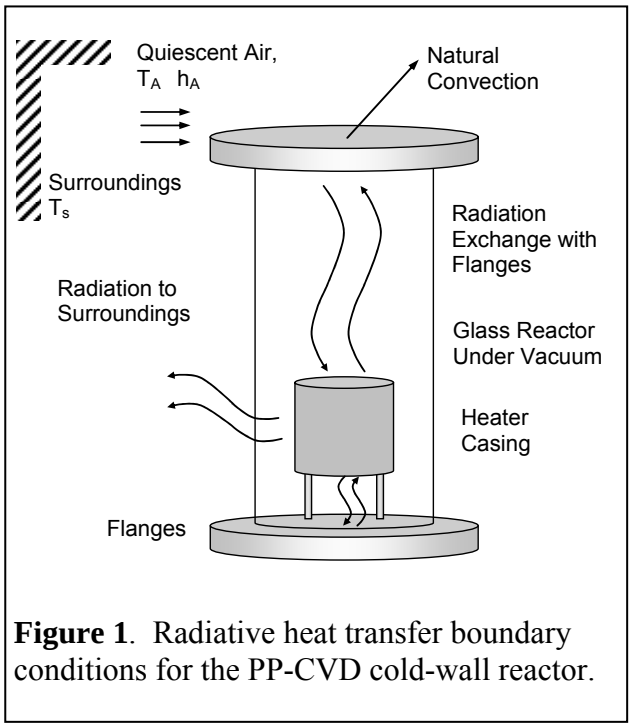

Figure 1. Radiative heat transfer boundary conditions for the PP-CVD cold-wall reactor.

$$\rho c \frac{\partial T}{\partial t} = -\nabla \cdot \{q\} + \ddot{Q} \qquad [1]$$

where ρ is the density, *c* is the specific heat, T is the temperature, ∇ is the spatial gradient operator, {q} is the heat flow rate vector, $\ddot{Q}$ is the internal heat generation rate per unit volume. The heat conduction inside the heater body is governed by the heat flow rate equation expressed for each isotropic solid. For constant thermal conductivity, **k** , the three-dimensional form of Fourier's Law is:

$$\{q\} = -\mathbf{k}\nabla T \qquad [2]$$

The general finite element expression of the thermal equilibrium equation applying the method of weighted residual (MWR) can be written:

$$[C]\{\dot{T}\} + [K_c]\{T\} = \{R_{\ddot{Q}}\} + \{R_q\} + \{R_h\} + \{R_r\} \qquad [3]$$

where, $[C]=\int \rho c[N][N]^T dV$ is the heat capacity matrix, $[N]$ is the shape function matrix, $[K_c]=\int k[B][B]^T dV$ is the heat conduction matrix, $\{T\}$ and $\{\dot{T}\}$ are the nodal temperature vector and nodal temperature rate vector, respectively, $\{R_{\ddot{Q}}\}$ and $\{R_q\}$ are the heat load vectors arising from internal heat generation and the surface heat flux, respectively, and, $\{R_h\}$ and $\{R_r\}$ are the heat flow vectors arising from surface convection and radiation, respectively (11).

In order to formulate and solve the radiant energy exchange problem, the radiation matrix method is adopted in the finite element analysis. The relationship between the energy losses and the surface temperatures is expressed by the energy balance for a system of *N* enclosures (12,13).

$$\sum_{i=1}^{N}\left(\frac{\delta_{ji}}{\varepsilon_i}-F_{ji}\frac{1-\varepsilon_i}{\varepsilon_i}\right)\frac{1}{A_i}q_i=\sum_{i=1}^{N}\left(\delta_{ji}-F_{ji}\right)\sigma T_i^4 \qquad [4]$$

where N is the number of radiating surfaces, δ_{ij} is the Kronecker delta, ε_i is the effective emissivity of surface i, F_{ij} is the radiation view factors, A_i is the area of surface i, q_i is the energy loss of surface i, σ is the Stefan-Boltzmann constant, and T_i the absolute temperature of surface i. To calculate view factors in the analysis, hidden method is used in this simulation since the heater surface is acting as a blocking surface between the surfaces of the flanges (13).

Using the matrix equation, Equation (4) can be represented with a single row as follows:

$$[C]\{Q\}=[D]\{T^4\} \qquad [5]$$

such that, each row j in $[C]=\left(\frac{\delta_{ji}}{\varepsilon_i}-F_{ji}\frac{1-\varepsilon_i}{\varepsilon_i}\right)\frac{1}{A_i}, i=1,2,...,N$ and each row j in $[D]=\left(\delta_{ji}-F_{ji}\right)\sigma, i=1,2,...,N$. Therefore, the radiation rate equation is linearized with the following radiation matrix form:

$$\{Q\}=[K']\{T\} \qquad [6]$$

$[K']$ includes T^3. Now, the energy loss is proportional to the temperature rather than to the temperature to the fourth power. The temperatures from the previous iterations are used to calculate $[K']$ and the solution is computed iteratively.

DESIGN OPTIMIZATION

The solution is subject to the assumptions that heat from the heater is only transferred by radiation effect to the flanges and surroundings (i.e., all of heat passes the glass tube). The reactor is considered to be an axial symmetry. The emissivity of the material used is not dependent on temperature. Heat conducted by the supporting legs of the heater is neglected because it is small compared with the total heat transfer from the heater casing by radiation.

The optimization design requirement, and thus the state variable, for the substrate heater is uniform temperature distribution at the heater surface. The optimisation problem can be generally represented as a constrained minimization problem whose aim is to minimize the objective function, $f = f(\mathbf{x}) - f^*$, where $\boldsymbol{f}(\mathbf{x})$ and $\boldsymbol{f}^*$ are the calculated state variable and desired state variable, respectively, calculated for each design variable, **x.** We used the first order optimization algorithm based on the derivatives for the objective function and the state variables.

The design optimization procedure used the FE-simulation to determine heater dimensions, L_1, L_2, L_3, L_4 as shown in Figure 2. A minimum temperature variation at the surface is used for the objective function using the constrained minimization problem:

$$\text{Minimize } f = \left|T_c - T_e\right| \quad \mathbf{x} = \left\lfloor L_1, L_2, L_3, L_4 \right\rfloor \qquad [7]$$

where T_c and T_e are the temperatures at the top center of the heater and at the edge, respectively. The ranges of the design variables to explore during the optimization process are listed in Figure 2. Using the optimal design, a subsequent optimization procedure was used to determine the heater power required to provide a deposition temperature of 550°C.

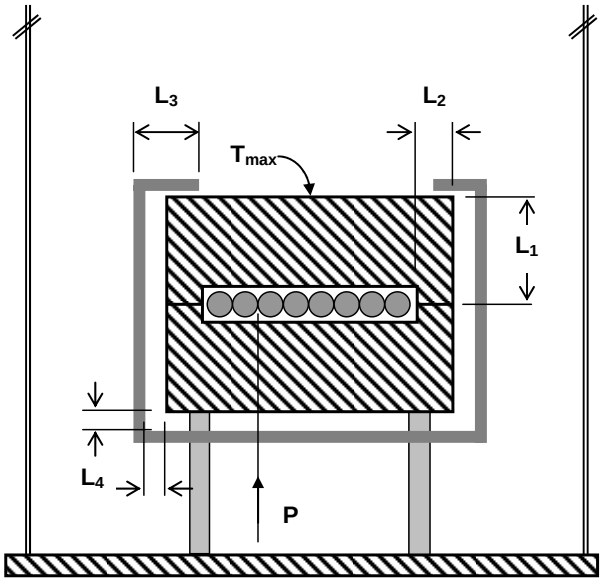

Design Optimization Parameters

L_1 = Thickness of upper heater stainless steel body
Range = 10 - 40mm

L_2 = Thickness of side wall stainless steel body around heating element
Range 1-6 mm

L_3 = Overhang length of stainless steel shield
Range = 5 – 20 mm

L_4 = Spacing between heater body and shield
Range = 10-20 mm

P = Electric power to the heater

T_{max}= Center point temperature

ΔT = Maximum temperature difference on heater surface

Figure 2. Basic cut view of the stainless steel (SUS 304) heater body with resistive element in the center. The dimensions to be optimized for the heater and shield are shown for the nominal 75mm diameter heater body.

EXPERIMENTAL

Thin film research usually involves deposition onto small substrate coupons using the commercial button heater. Our experience is that the button surface has un-even heating and temperature, and given that it is so expensive, we take big risks cleaning extraneous deposition off the heater. A metal heater that is robust and easily disassembled for cleaning would have certain functional advantages.

We constructed four very simple solid stainless heaters. The main body has two matching pieces of stainless steel with a low cost resistive heating element clamped between them. Two thicknesses for the top half were modelled and tested. A simple shield of 5mm thickness machined from stainless steel was then constructed around the sides and base of the stainless heater. Finally, a shield casing was used, according to the dimensions determined in the optimization analysis. The experimental stainless heaters are model CVD heaters only, where the simple geometry and heat transfer conditions allow us to verify the ANSYS modelling of the materials, boundary conditions, and assumptions. The model heaters were used to study the effect of various geometrical dimensions and shielding configurations on heater surface uniformity.

The power input was set at 100W for the first four configurations, and the temperature controller was set at 550^{o}C for the final experiment. The average power input is measured with the digital power meter. The reactor is maintained at 10^{-3} Torr vacuum until steady state temperature is achieved. Then the top flange was removed and the temperature profile of the susceptor surface and walls was recorded using a digital IR camera, Land Cyclops Ti814, and a shielded surface probe thermocouple.

RESULTS

The numerical results showed an improvement of surface temperature uniformity with increased heater top thickness. The temperature uniformity was further improved with shielding. Table 1 gives the heater dimensions from the numerical optimization. The optimal heater design was predicted to have less than four degree radial temperature variation.

Table 1. Results of optimization.

Design Variable	Optimized Value
L_1	30 mm
L_2	3 mm
L_3	7 mm
L_4	18 mm

The thermography results showed reasonable agreement with the numerical simulation. Figure 3 gives a summary of the model heater dimensions and features, ANSYS simulation results, temperature probe measurements at the top center, and thermography analysis of the temperature uniformity. Figure 4 shows the thermograph of the optimal heater top, a radial temperature profile, and surface temperature histogram. The outside shield temperature predicted in the simulation was also verified. With the shielded configuration, the temperature of all surfaces other than the substrate would be well below the deposition temperature.

CONCLUSION

We investigated the relationship between heater body geometry and surface temperature uniformity for a two-inch wafer heater in a cold-wall reactor. Stainless steel construction and a resistance coil heater were used for robust operation, in-house manufacture, and most importantly, low cost. Project objectives are to minimize cost, and maximize process control and efficiency. The PP-CVD system uses conduction substrate heating in a cold-wall reactor with pressure pulsing between 1Pa and 40 kPa several times per minute. We found that design and performance of CVD heaters is not well covered in handbooks or research literature. Commercial heaters are very expensive, and designed for PVD.

Configuration		Simulation [^{o}C]		Experiments [^{o}C]	
1	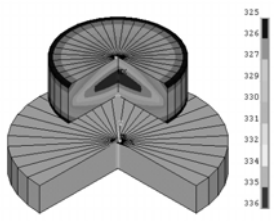 Unshielded, 25mm thick	P = 100W T_{max} = 331 T_{min} = 325 T_{htr}= 336	Surface ΔT = 6 Side T_{max} =331	T-couple T_{probe} = 335 Side T_{max} = 260	IR Image T_{mean}= 272 ΔT = 13 σ = 6.6
2	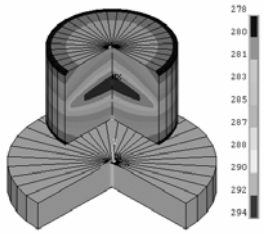 Unshielded, 50mm thick	P = 100W T_{max} = 284 T_{min} = 279 T_{htr}= 294	Surface ΔT = 5 Side T_{max} =284	T-couple T_{probe} = 280 Side T_{max} =260	IR Image T_{mean}= 272 ΔT = 6 σ = 3.4
3	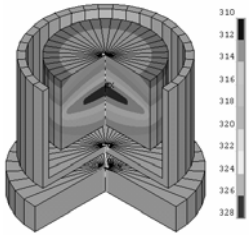 Simple Shield, 50mm thick	P = 100W T_{max} = 317 T_{min} = 313 T_{htr}= 328	Surface ΔT = 4.6	T-couple T_{probe} = 368 Shield T_{max} = 130	IR Image T_{mean}= 317 ΔT = 6 σ = 2.6
4	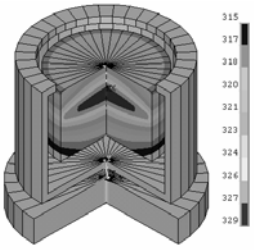 Optimal Design, 50mm thick	P = 100W T_{max} = 331 T_{min} = 327 T_{htr}= 329	Surface ΔT = 4	T-couple T_{probe} = 376 Shield T_{max} = 137	IR Image T_{mean}= 325 ΔT = 8 σ = 4
	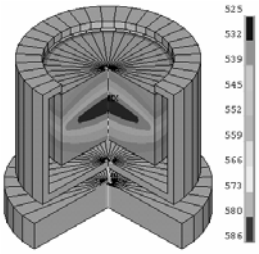 Optimal Design at 550^{o}C	P = 385W T_{max}= 550 T_{htr}= 586	Surface ΔT = 13	T-couple T_{probe} = 665 Shield T_{max} = 315	IR Image Outside range

Figure 3. Numerical simulation of each heater configuration with maximum surface temperature, T_{max}, and uniformity, ΔT, from the ANSYS model compared to the probe measurements and thermography analysis.

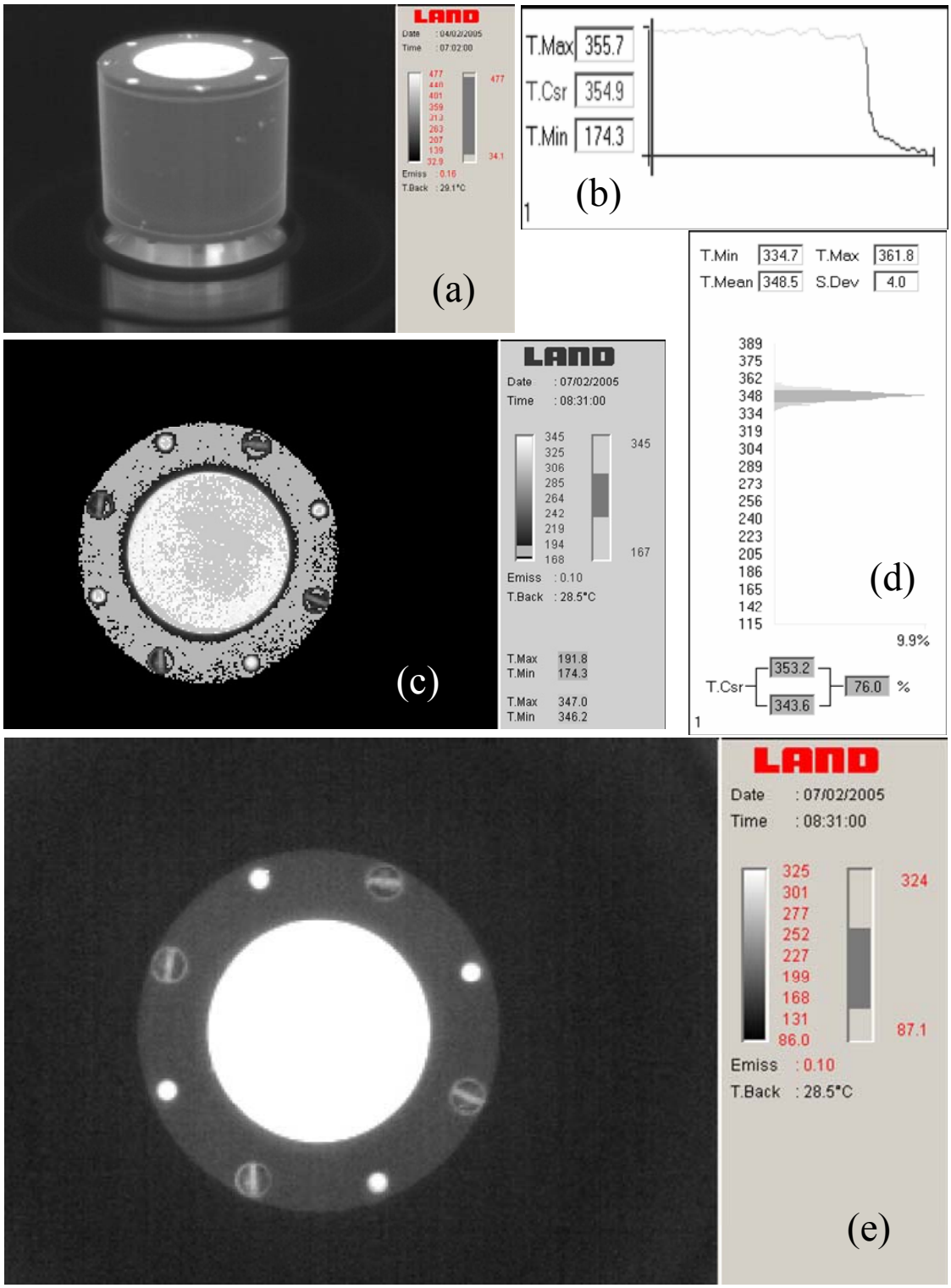

°C and side temperature 175°C at 100W power. (a) side view, (b) radial temperature profile, (c) isotherm pixel enhancement showing a 2° temperature band on the surface, (d)histogram of heater surface, (e) thermal image of top polished stainless steel surface.

The three-dimensional heat conduction equation was solved for the reactor body using the finite element modelling package, ANSYS, subject to radiation boundary conditions. The optimization approach, based on the derivative of the objective function given in Eqn. 7, was used to determine the optimal dimensions. The optimal design had a thick stainless steel layer between the heating element and the heating surface, and shielding around the sides and top edge. The thick top seems to run counter to commercial heater design, which tends toward ceramic or radiant heating elements where the substrate is either placed directly on the heating element or a very thin top is used as a radiant diffuser. However, the superior temperature uniformity of the thick material is explained by the refractory properties of the material. Many of the processing temperatures for MOCVD processes do not exceed the service temperature for stainless steel, so the design was considered feasible.

Four stainless heater configurations were constructed and modelled. The steady state surface temperature profile was measured by infrared camera and surface probe thermocouple. The finite element model solution was in reasonable agreement with the experimental measurements for 100W power input. Unshielded heater configurations had the worst temperature uniformity, but a thicker top improved the uniformity. Shielding the body of the heater increased the surface temperature and increased the uniformity. The optimal design had a shield on the sides and bottom, and also around the top corners of the heater body, giving steady state temperature uniformity of $\Delta T = 4^{o}C$. The commercial alumina button heater cost in excess of $1200 USD, in contrast to our stainless heater with resistance element which cost less than $200 USD.

REFERENCES

1. M. Ohring, *Materials Science of Thin Films*, Academic Press, San Diego (2002).
2. D.I. Fotiadis, M. Boekholt, K.F. Jensen, and W. Richter, *Journal of Crystal Growth,* **100,** 577 (1990)
3. E.O. Einset, D.I. Fotiadis, K.F. Jensen, T.F. Kuech, p 38, Proceedings of The Electrochemical Society, v 90, n 12, (1990)
4. M.L. Hitchman and K.F. Jensen, *Chemical Vapor Deposition*, Academic Press, London (1993).
5. D. L. Smith, *Thin Film Deposition*, p. 200, McGraw Hill, Boston (1995).
6. E. Lugscheider, C. Barimani and G. Dőpper, *Surface & Coatings Technology*, **98,** p.1221 (1998).
7. R. Campion, R.G. Ormson, C.A. Bashford and P.J. King, Design and performance of a reliable and low cost substrate heater for superconducting thin film deposition, *Vacuum*, **46** No.2 (1994) 195-197.
8. E.E. Inameti, M.S. Raven, Y.M. Wan and B.G. Murray, *Vacuum*, **43**, 121 (1992).
9. US Patent No. 5,451,260. CRF D-1394-Raj, *et al* Sono-Tek Corp. (1986).
10. V.S. Arpact, *Conduction Heat Transfer,* Addison-Wesley Publishing (1966).
11. K.H. Huebner, D.L. Dewhirst, D.E. Smith, and T.G. Byrom, *The Finite Element Method for Engineers*, Wiley & Sons, Inc. (2001).
12. R. Siegal and J.R. Howell, *Thermal Radiation Heat Transfer*, Hemisphere Publishing Corp. (1981).
13. AYSYS Theory Manual, Release 8.0, ANSYS Inc. (2004).